ACS OMEGA

Open Access

http://pubs.acs.org/journal/acsodf

Article

Research on the Biogas Production Mechanism of Mudstone in the Qaidam Basin under Different CO_2 Pressures

Hongna Song, Hang Lv, Daping Xia,* and Jixian Tian

Cite This: *ACS Omega* 2024, 9, 40559−40565

Read Online

ACCESS | Metrics & More | Article Recommendations

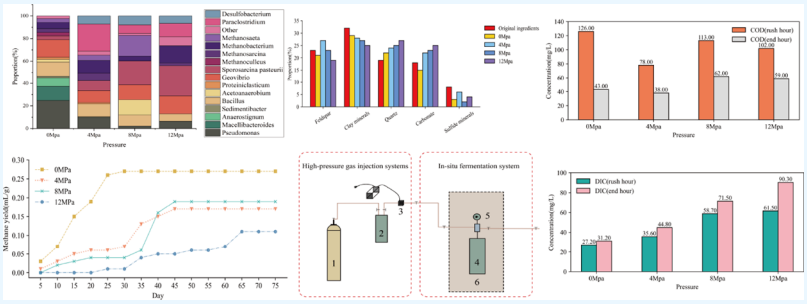

ABSTRACT: Mudstone, a class of sedimentary rocks rich in organic matter, possesses considerable potential for biogas production. Mudstones possess a rich biological origin, which is conducive to refining the mechanisms and enrichment patterns of biogenic gas reservoirs. This has significant theoretical and practical implications for guiding the exploration and development of Quaternary mudstone gas reservoirs. Furthermore, the Qaidam Basin is an excellent place for the geological storage of CO_2 due to its rich petroleum reservoir conditions. Experimental research on biogas production under diverse CO_2 pressure−mudstone−microorganism−water interactions is conducted to determine the biogas production mechanism of mudstone under different CO_2 pressures during sequestration circumstances. According to the results: (1) under supercritical carbon dioxide conditions, there is a slight initial increase in biogas production, followed by a gradual decrease. The periods and peaks of gas production vary among the different reaction groups. As carbon dioxide pressure increases, the gas production cycle lengthens significantly, while the gas yield declines. (2) Siderite and secondary carbonate minerals have increased in the mudstone's mineral fraction both before and after biogas production, while clay mineral groups have decreased. Specifically, there was a notable drop in chlorite and kaolinite. (3) Microorganism species in the system were analyzed, and the results showed that there was a gap in each microorganism's ability to adapt to its surroundings, and the diversity and quantity of bacteria declined with increasing pressure. After carbon dioxide was fluxed, there was a considerable shift in the pattern of biogas generation, which consequently had a major impact on the alterations in mineral fractions.

1. INTRODUCTION

Ever since General Secretary Xi Jinping put forth the dual-carbon target in September 2020, the concept and objective of geological carbon dioxide storage have steadily gained clarity.[1] Coalbed methane replacement, oil and gas reservoir storage, and saltwater layer storage are the three directions of CO_2 geological storage.[2,3] The first involves the collection of large amounts of CO_2 from flue gases released by emission sources by CO_2 capture devices, which are then injected into geological formations such as underground oil and gas fields to be used for coalbed methane replacement and improving oil and gas recovery. At the same time, deltaic facies evolved in the Charkhan and Salt Lake areas, and shallow to semideep lakes developed in the Pliocene to Quaternary periods in Sebei, Sedong, and Jinda.[4−6] The lithology of the samples is primarily composed of silty mudstone and mudstone with a small amount of carbonaceous mudstone. The organic matter of the samples is primarily sourced from the input of terrestrial vascular plants, complemented by contributions from lower aquatic organisms. With a strong carbon dominance index (CPI), the carbon chain length distribution of *n*-alkanes varies from C_{10} to C_{33}, suggesting that the sample is immature. Some of the samples appear to be even-carbon dominating based on the OEP values, which could indicate that they are derived from organic matter found in saltwater.[7−9] There are not enough hydrocarbons with a low molecular weight. The Qaidam Basin is also one of the places with the most potential for CO_2 storage in China, and the

Received: April 27, 2024
Revised: July 31, 2024
Accepted: August 1, 2024
Published: September 23, 2024

TN18 well obtained an industrial gas flow in a mudstone formation, producing up to 2×10^4 m^3 of gas per day. Over 3400 m of thickness and 6000 m^2 make up the Quaternary mudstone development in the Sanhu region of the Qaidam Basin. Mudstone-hosted biogas reservoirs exhibit a wide range of material substrates, which form a fundamental basis for their formation and potential exploration.

With an average organic carbon content of 0.32% and a typical range of 0.25 to 0.56%, the Quaternary mudstones show a comparatively low abundance of organic matter. The chloroform asphalt A content typically ranges from 0.005 to 0.04%, with an average value of 0.016%. The total hydrocarbon content ranges from 20 to 100 μg/g, with averaging 80 μg/g. The vitrinite reflectance (Ro), typically between 0.25 and 0.45%, indicates an immature stage. In the Quaternary period, microorganisms mainly consist of sulfate-reducing bacteria, cellulose-degrading bacteria, and fermenting bacteria, prevalent from shallow to deep layers.[10−13] Among archaea, methane-producing archaea dominate, including widespread genera such as Methanobacterium, along with rod-shaped, coccus, and bacillus forms.[14]

During the geological sequestration process, the injected carbon dioxide can displace oil, gas, and coalbed methane.[15] It can also interact biochemically with the coal and organic sedimentary rocks within to alter the conditions in which microorganisms survive.[16−18] This could indirectly limit the potential of producing biogas from mudstone.[19]

To investigate the response mechanism of mudstone for biogas production potential in the process of CO_2 sequestration under various pressure conditions, four different pressure conditions (0, 4, 8, and 12 MPa) were designed. The experiments were conducted by enriching the mudstone's microbial nutrient solution components in an autoclave, with a pumping tube to function as the gas collection device. The reaction time was set at 60 days, allowing for analysis of the microbial community distribution, mudstone state, intermediate liquid phase parameters, and gas production before and after the reaction. The reaction mechanism was clarified.[20−22]

2. EXPERIMENT

2.1. Experiment Preparation. Using a grinder, 200 g of fresh rock powder was ground to enrich the native microorganisms in the mudstone using the mixing and suspension method. As demonstrated in Table 3, enrich the mixture in an incubator for 7 days until it reaches a volume of 1000 mL, and then, another 200 g of fresh rock powder, which will be placed in an autoclave, is used to ensure that the experiments are repeatable and reproducible. The samples are used in three parallel samples connected to the periphery of the carbon dioxide cylinders. The carbon dioxide one-time pass is depicted in Figure 1.

Enrichment of nutrient solution components:

(1) NH_4Cl: 1.0 g/L, (2) $K_2HPO_4{\cdot}3H_2O$: 0.4 g/L, (3) KH_2PO_4: 0.2 g/L, (4) sodium acetate: 1.0 g/L, (5) sodium formate: 1.0 g/L, (6) *Saccharomyces cerevisiae*: 1.0 g/L, (7) pancreatic digest of casein: 0.1 g/L, (8) $MgCl_2{\cdot}6H_2O$: 0.1 g/L, and (9) trace element solution: 10 mL/L.

2.2. Test Methods. *2.2.1. Microbial High-Throughput Sequencing.* The liquid phase product samples were sent to Shanghai Meiji Biomedical Technology Co for high-throughput sequencing of bacteria and archaea to identify microbial diversity. Following DNA extraction using FastDNASpinkit, 1% agarose gel electrophoresis was performed to visualize and confirm the integrity of the extracted genomic DNA. Following that, PCR amplification was carried out using TransGenAP221-02: TransStartFastpfuDNAPolymerase and particular primers with barcodes were created following the specified sequencing region; PCR instrument: ABIGeneAmp®9700; all samples were analyzed according to the official experimental conditions of Henan Polytechnic University (HPU), and the PCR products from the same samples were mixed and detected by 2% agarose gel electrophoresis. PCR products were quantified by Quanti-Fluor-ST Blue Fluorescence Quantification System (Promega) based on the preliminary quantification results of electrophoresis.

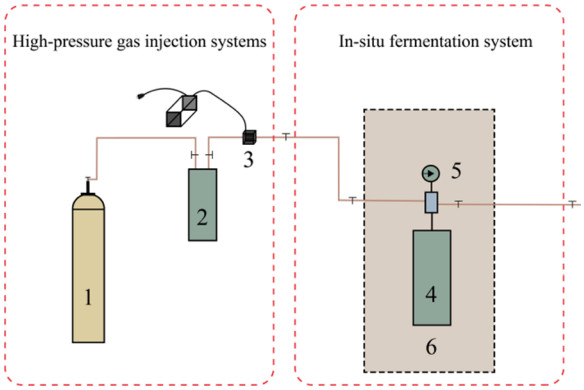

Figure 1. Experimental setups.

2.2.2. Organic Geochemical Signature Detection. Tests were carried out on six parameters: pyrolysis, Ro, hydrogen index, chloroform asphalt A, and mudstone TOC. The specific geochemical indices tested are shown in Tables 1 and 2 alongside the primary mineral fractions.

Table 1. Geochemical Indicators of Mudstones[a]

	TOC	HI	chloroform asphalt A	R_0	S1/S2
mudstone	0.35	133	123×10^{-5}	0.2	1.53

[a]Note: Unit is wt % for TOC, mg HC/g TOC for HI, % for chloroform asphalt A, and % for R_0.

Table 2. Primary Mineral Fractions of Mudstone

	feldspar	clay minerals	quartz	carbonate	sulfide
mudstone	23%	32%	19%	18%	8%

2.2.3. XRD Monitoring Methods for Minerals. X-ray diffraction (XRD) analysis was performed by utilizing a Shimadzu XRD-6100 spectrometer. The sample underwent a rigorous preparation process, including drying, pulverization, and sieving through a 200 mesh sieve to achieve a fine, uniform

Table 3. Gas-Producing Group

pressure (MPa)	experimental group	temperature (°C)	number
0	200 g rock sample + 2000 mL enriched bacterial solution	35	M1
4	200 g rock sample + 2000 mL enriched bacterial solution	35	M2
8	200 g rock sample + 2000 mL enriched bacterial solution	35	M3
12	200 g rock sample + 2000 mL enriched bacterial solution	35	M4

https://doi.org/10.1021/acsomega.4c04022
ACS Omega 2024, 9, 40559−40565

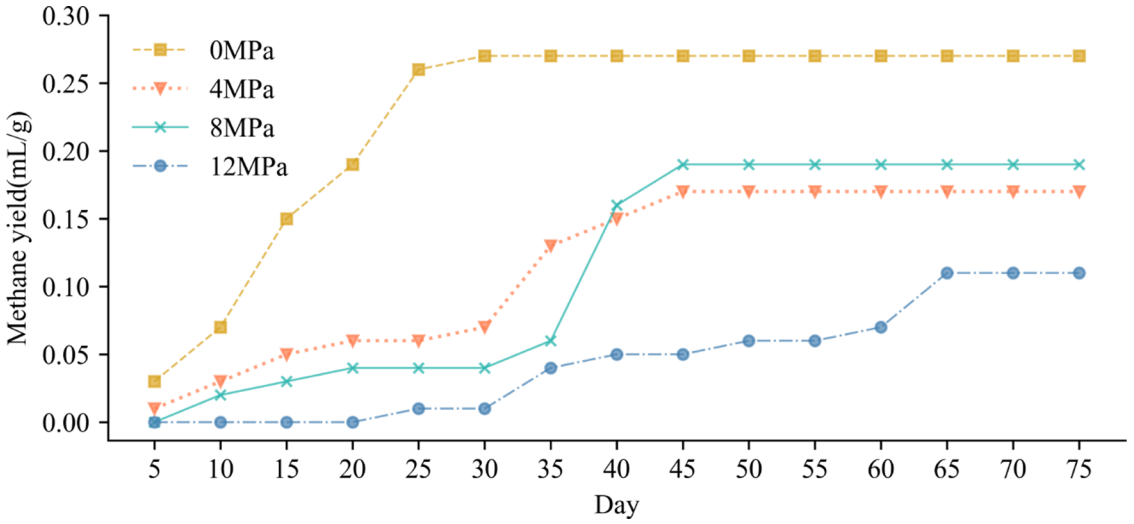

Figure 2. Cumulative gas production at different pressures.

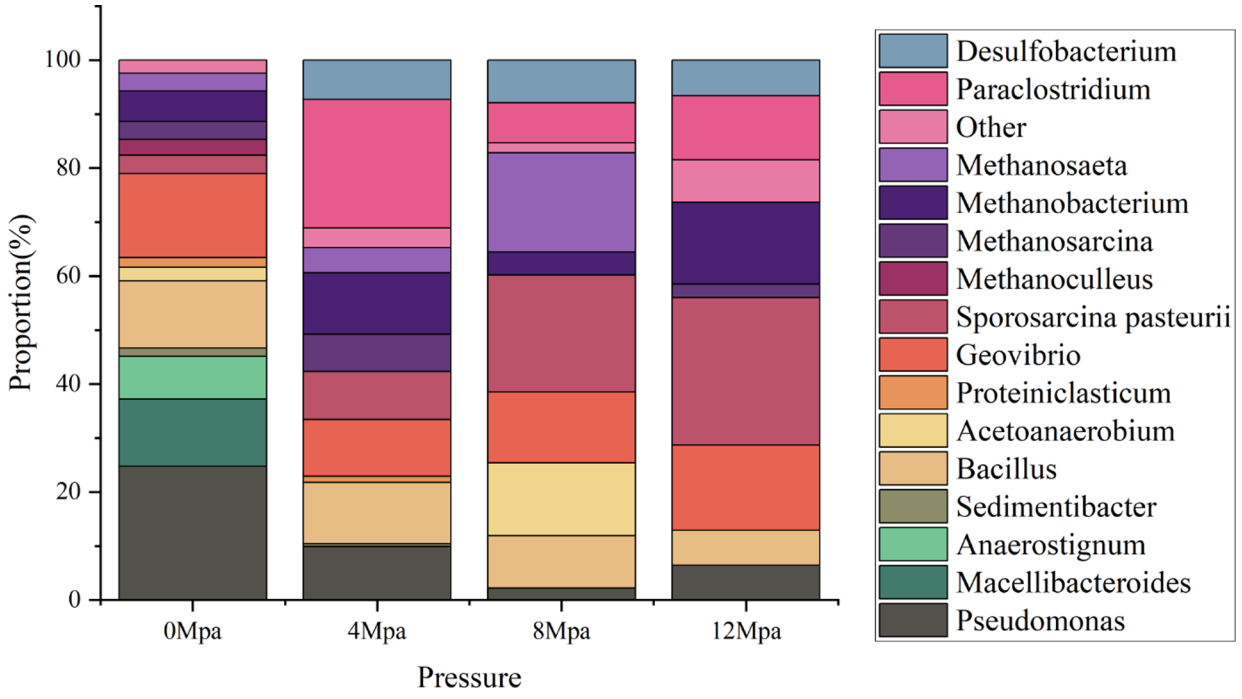

Figure 3. Distribution of flora at different pressures.

powder. The resultant powder was carefully deposited into the sample holder's recess, ensuring a flat and even distribution across the surface of the sample holder. Subsequently, the sample holder was meticulously positioned within the spectrometer's sample chamber, with the protective enclosure securely closed to maintain optimal experimental conditions. The XRD scan was conducted over a range of 2θ angles from 5° to 80°, with a scanning rate of 4°/min to ensure comprehensive data acquisition. The acquired diffraction patterns were subjected to qualitative and quantitative mineral analysis using the advanced MDI Jade 6.0 software, facilitating a precise characterization of the sample's mineral composition.

3. ANALYSIS OF THE RESULTS

3.1. Gas Production Results Analysis. Figure 2 illustrates the significant disparity in gas production from mudstone under various CO_2 conditions. In the absence of CO_2, the maximum gas production reached 0.27 mL/g, after which the production declined. Upon reaching the supercritical condition at 8 MPa, there was a slight increase in gas production to 0.19 mL/g, followed by a continuous decrease. The peak gas production period and the production cycle varied among the groups; the higher the CO_2 content, the longer the production cycle, with the initial gas production time being postponed and the peak production period arriving later. For the M4 sample group, the production cycle extended to 70 days with a short duration of peak production and a weak gas production capacity, resulting in a final total gas production of only 0.06 L/g. In contrast, the total gas production time at 0 MPa was 30 days, which was 40 days earlier than that of the M5 group. This outcome significantly deviates from the gas production results of many previously studied samples.[23,24]

https://doi.org/10.1021/acsomega.4c04022
ACS Omega 2024, 9, 40559−40565

3.2. Microorganism Species Analysis. As depicted in Figure 3, the microbial populations in the reacted system were classified, and it was discovered that there were significant differences among the types of microbial populations under various carbon dioxide pressures. The diversity of microorganisms peaked at 0 MPa, and after that, both the abundance and diversity of microorganisms declined, and the community structure changed more visibly. *Pseudomonas, Sedimentibacter, Proteiniclasticum, Acetoanaerobium*, and other significant functional bacteria with hydrolysis effects in M1 and M2 gradually decreased in abundance. As the pressure increased and the solution acidified, the Slaughterhouse rod *Macellibacteroides* is no longer present in M4. However, several genera of bacteria are still present in some amounts, including Bacteroidales, Petrimonas, Aminobacterium, Paraclostridium, *Sporosarcina pasteurii*, and *Bacillus*. About these, *Paraclostridium*'s abundance within bacterial genera increased initially before declining. It is also a valuable member of the hydrolyzing bacterial flora class, which is responsible for breaking down some of the macromolecules involved in the decomposition of organic matter. Furthermore, *Paraclostridium* exhibits a high degree of acid tolerance, allowing it to persist and fulfill its function in situations where the carbon dioxide pressure is higher and the solution is acidic. With its ability to quickly manufacture additional carbonate, *Sporosarcina pasteurii* can produce precipitates of $CaCO_3$ and $MgCO_3$, which can partially clog pores in the rock and reduce its porosity. This is also the cause of the later increase of secondary carbonate minerals.

Additionally, genus types revealed that the Geobacillus and Methanobacterium of bacterial and archaeal community species become more abundant under increasing pressure, indicating that the bacillus strains were more carbon dioxide tolerant. These align more closely with earlier research findings.[25]

Within the CO_2−water−microorganism−mudstone system, some minerals of the mudstone are prone to dissolution or migration, which can partially counteract environmental changes within the system. Consequently, certain microorganisms may adapt to the extreme conditions of increased CO_2 pressures, ultimately evolving into a new dominant microbial flora.

Considering the operational taxonomic unit (OTU) counts of bacteria and Archaea, as well as the changes in the Shannon−Wiener diversity index, it is evident that as the pressure of CO_2−water−microbial interactions increases, the diversity of bacteria and archaea declines, the community structure tends toward homogeneous, and the abundance declines in real time. However, the bacterial community, which includes a greater number of genera, tends to have species that are more resilient to environmental changes compared to the species of Archaea.

3.3. pH, COD, DIC, and Other Relevant Parameters in Solution. As illustrated in Figures 4, 5, and 6, the pH values exhibit a progressive decline with an escalation of carbon dioxide concentrations. Specifically, the pH in the M4 group has reached a critical threshold of 5.8, which is notably acidic and potentially detrimental to the proliferation of microorganisms accustomed to neutral environments. This acidic pH could precipitate the demise of a substantial fraction of bacteria that preferentially thrive under neutral conditions. Conversely, the M1 group demonstrates a relatively stable pH, consistently hovering around 6.8. Interestingly, despite the higher acidity, the COD values in the M4 and M5 groups have paradoxically increased relative to earlier groups. This enhancement may stem from the augmented solubility of minerals in the solution due to increased

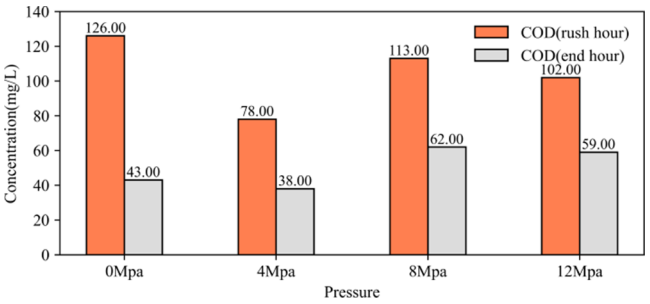

Figure 4. COD results under different pressures.

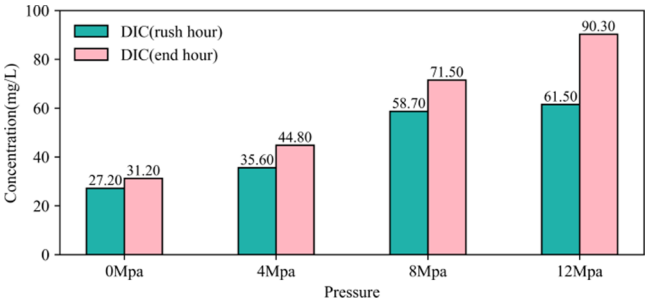

Figure 5. DIC results under different pressures.

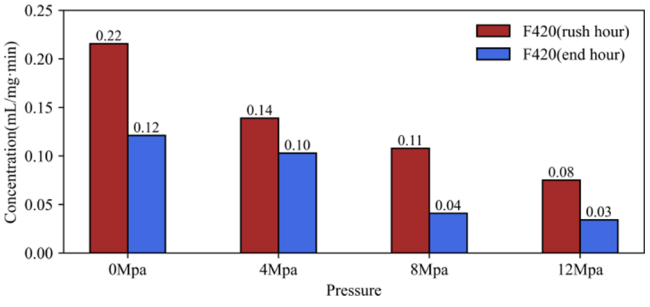

Figure 6. F420 results under different pressures.

acidity, as well as the partial degradation of more recalcitrant fractions of organic carbon, thereby augmenting the COD content within the solution. Additionally, the DIC values have also been observed to escalate, diverging from the conclusions of prior research that typically report a postreaction decrease in DIC concentration. This discrepancy may be attributed to two primary factors. On one hand, the introduction of carbon dioxide into the aqueous environment leads to an accumulation of bicarbonate ions. On the other hand, the reduction in pH facilitates the partial dissolution of carbonate minerals within the mudstone, culminating in a more pronounced elevation of the total bicarbonate ion concentration in the solution.

3.4. Variation of Geochemical Parameters in Mudstone. By examining the variations in the geochemical parameters of the mudstone that had reacted, it was possible to determine that the total TOC had decreased after the reaction. The reduction in organic carbon was proportional to the increase in pressure, as part of the organic carbon was consumed by the microbial degradation process. However, the reduction in organic carbon did not increase gas production. The organic carbon will partially dissolve in the acidic solution due to the increased pressure, and once supercritical conditions are reached, carbon dioxide also has an extractive effect, causing the organic matter in the mudstone to be extracted into the reaction solution. However, the amount of change that occurs

https://doi.org/10.1021/acsomega.4c04022
ACS Omega 2024, 9, 40559−40565

Table 4. Gas-Producing Group

	TOC (wt %)	HI (mg HC/g TOC)	chloroform asphalt A (%)	R0 (%)	free and cracked hydrocarbons S1 + S2
original ingredients	0.35	133	127×10^{-5}	0.2	1.53
0 MPa	0.27	89	133×10^{-5}	0.2	1.45
4 MPa	0.29	92	117×10^{-5}	0.2	1.21
8 MPa	0.33	104	123×10^{-5}	0.2	1.38
12 MPa	0.34	113	128×10^{-5}	0.2	1.33

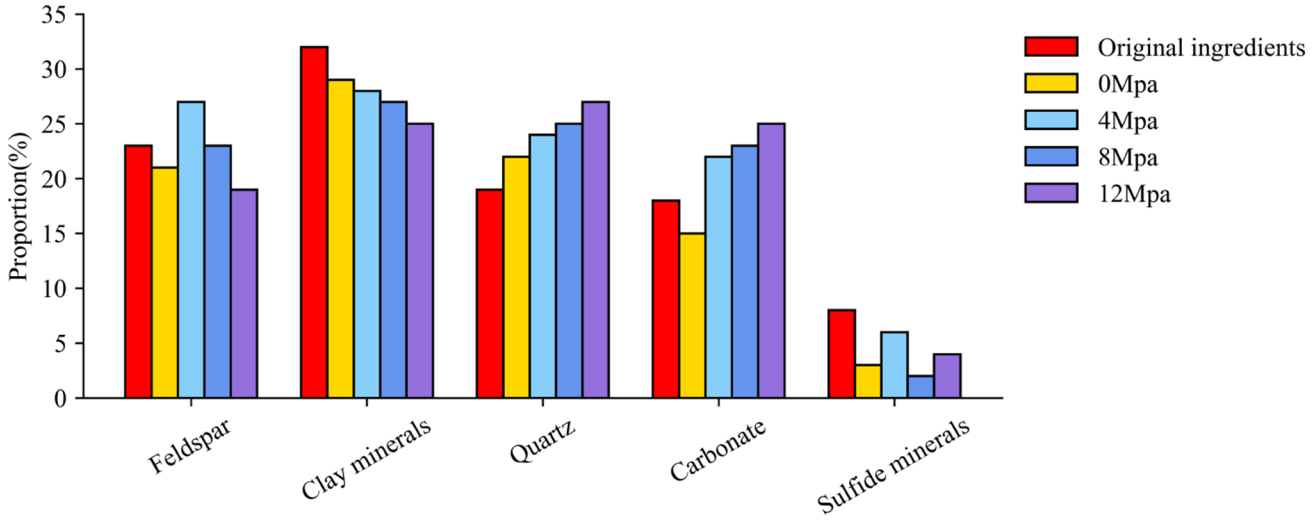

Figure 7. Compositional changes at different pressures.

after the pressure is increased is relatively small, even though the amount of organic carbon is reduced. From the change of chloroform asphalt A, the amount of chloroform asphalt A of 0, 8, and 12 MPa changed more, and 0 MPa < 8 MPa < 12 MPa, 4 MPa did not decrease. The primary cause of the change in organic carbon trend is that chloroform asphalt A is a more active component in mudstone; under 0 MPa, microbial activity is primarily higher and there is more degradation of the component; at 8 and 12 MPa, the change in chloroform asphalt A is still because it is easier to extract (Table 4).

3.5. Mineral Changes in Mudstone after Reaction. As shown in Figure 7, when mudstone mineral components under different pressure conditions are compared to their changes before and after gas production, it is observed that the degree of change in mudstone mineral components varies under different pressure conditions. Among these, the carbonate mineral components increased more visibly, feldspar minerals showed a decreasing trend, and the content of clay minerals increased in the initial stages; however, the clay mineral components also showed a decrease after reaching supercritical conditions. The change in the sulfide mineral types is not readily apparent. As pressure rises, the carbonate minerals rise more, some metal elements in the feldspar and clay minerals dissolve, the feldspar minerals decrease more as a result of greater dissolution, and the clay minerals decrease initially. In both type (2) and type (3) dissolution reactions, carbonate ions combine with metal ions to form new carbonate minerals. Furthermore, a portion of these metal ions recombine with silicic acid to form clay minerals. These newly formed minerals are classified as secondary and they reattach to the surface of the original minerals.

$$CO_2 + H_2O \leftrightarrow H_2CO_3(aq)$$

$$H_2CO_3(aq) \leftrightarrow H^+ + HCO_3^-$$

$$HCO_3^- \leftrightarrow H^+ + CO_3^{2-} \quad (1)$$

$$M + CO_3^{2-} \leftrightarrow MCO_3(s) \quad (2)$$

$$Mg_{2.964}Fe_{1.927}Al_{2.483}Ca_{0.011}Si_{2.633}O_{10}(OH)_8 + 17.468H^+ \leftrightarrow 2.483Al^{3+} + 0.011Ca^{2+} + 1.712Fe^{2+} + 2.964Mg^{2+} + 2.633H_4SiO_4(aq) + 0.215Fe^{3+} + 7.468H_2O \quad (3)$$

3.6. Discussion. Within biogas production reactions in mudstone subjected to varying CO_2 pressure conditions, it is evident that an increase in pressure within the CO_2−microbe−water−mudstone system results in a gradual decrease in gas yield and a corresponding elongation of the gas production cycle. As the pressure increases, the pH value in the liquid phase gradually decreases, the concentration of VFA decreases, and the concentration of DIC increases. Despite the enhanced solubility when CO_2 reaches its supercritical state, the increased dissolution of COD in the liquid phase indicates heightened solubility of organic matter and chloroform asphalt A after the reaction. The microbial community structure shows decreased diversity and abundance as pressure rises, along with an enrichment of pressure- and acid-tolerant bacteria and archaea. Notably, species such as Desulfobacillus, Methanobacillus, and Geobacillus become more abundant. This adaptation likely indicates that the microbial community requires extended periods under gas and pressure conditions to achieve optimal adaptation and reestablish stability. Enzymes essential for the generation of methane, such as hydrogenase and F420, also diminish concurrently, suggesting a general decrease in the metabolic activity of microbes. Reduced capacity for COD degradation weakens the solution reactivity, leading to a notable

https://doi.org/10.1021/acsomega.4c04022
ACS Omega 2024, 9, 40559−40565

reduction in the diversity of chemical reactions. Mudstone's mineral composition is dramatically changed by CO_2 dissolution following the reaction, especially with the increase of carbonate minerals. Analyses suggest that carbonate minerals are involved in dissolution−precipitation reactions, leading to the formation of secondary minerals, while a minor dissolution of clay minerals leads to the formation of new clay minerals. This process releases metal ions, which may contribute to the decline in the microbial activity.

4. CONCLUSIONS

This study conducted simulated in situ biogas production experiments for carbon dioxide sequestration in mudstones from the Qaidam Basin, highlighting the potential for biogas generation. High-throughput sequencing data reveal significant activity of cellulolytic and proteolytic bacteria, acidophilic bacteria, and methanotrophic bacteria at depths ranging from 1250 to 1750 m, indicating the presence of abundant substrates necessary for methane production in this stratum. The conclusions drawn from gas production results under various pressure conditions are as follows:

1. The higher the CO_2 pressure, the lower the biogas production and the longer the biogas production cycle; the maximum unit gas yield of mudstone at 0 MPa is 0.27 mL/g.
2. With increasing carbon dioxide pressure, microbial metabolic activity gradually decreases, and the dominant communities shift to more acid- and pressure-tolerant genera, resulting in an extended biogas production cycle.
3. As pressure increases, the mineral composition of mudstone changes significantly, with a notable increase in carbonate minerals, an initial increase followed by a decrease in clay minerals, and a gradual reduction in feldspar minerals. Additionally, the contents of TOC and chloroform asphalt A are reduced.

AUTHOR INFORMATION

Corresponding Author

Daping Xia − *Institute of Energy Science & Engineering, Henan Polytechnic University, Jiaozuo 454000, China; Collaborative Innovation Center of Coal Work Safety and Clean High Efficiency Utilization, Jiaozuo 454000, China; Henan Province Coal Mine Rock Strata Control International Joint Laboratory, Jiaozuo 454000, China*; Email: xiadp22@hpu.edu.cn

Authors

Hongna Song − *Institute of Business Administration, Henan Polytechnic University, Jiaozuo 454000, China*

Hang Lv − *Institute of Resources & Environment, Henan Polytechnic University, Jiaozuo 454000, China*; orcid.org/0000-0002-7319-6994

Jixian Tian − *Research Institute of Petroleum Exploration and Development - Langfang Branch, Langfang 065000, China*

Complete contact information is available at: https://pubs.acs.org/10.1021/acsomega.4c04022

Author Contributions

H.S. designed the experiment and wrote a manuscript, H.L. organized and analyzed the data, D.X. provided the experimental equipment, and J.T. provided technical support.

Funding

National Natural Science Foundation of China (42172199). Henan Province Soft Science Research (242400410473). Henan Province Education Science Planning (2023YB0071). Henan Polytechnic University Doctoral Fund (SKB2022−12). Key Laboratory of Coalbed Methane Resources and Reservoir Formation Process of the Ministry of Education (China University of Mining and Technology) (No. 2022-003).

Notes

The authors declare no competing financial interest.

ACKNOWLEDGMENTS

The authors acknowledge funding from the National Natural Science Foundation of China (42172199), the Henan Province Soft Science Research (242400410473), the Henan Province Education Science Planning (2023YB0071), and the Henan Polytechnic University Doctoral Fund (SKB2022-12).

REFERENCES

(1) Li, D.; Su, X.; Su, L. Theory of gas traps in stope and its application in ground extraction of abandoned mine gas:Part 2 − The develop ment suitability evaluation of gas trap and its application. *J. Pet. Sci. Eng.* **2022**, *208*, No. 109286.

(2) Shuangming, W.; Yanjun, S.; Qiang, S.; et al. Under ground CO2 storage and technical problems in coal mining area under the "dual carbon" target. *J. China Coal Soc.* **2022**, *47* (1), 45−60.

(3) Zhijian, H.; Ru, L.; Zhi, C. Strategic thinking on the ecologicaldevelopment of technology under china's "carbon neutrality" commitment. *Forum on Science and Technology in China* **2021**, *5*, 14−20.

(4) Caineng, Z.; Yanpeng, C.; Bo, X.; et al. Mission of new energy under carbon neutrality goal in China. *Bull. Chin. Acad. Sci.* **2023**, *38* (1), 48−58.

(5) Sacuta, N.; Daly, D.; Botnen, B.; Worth, K. Communicating about the geological storage of carbon dioxide-comparing public outreach for CO2 EOR and saline storage projects. *Energy Procedia* **2017**, *114*, 7245−7259.

(6) Carman, C. H.; Blakley, C. S.; Korose, C. P.; Zimmerman, J.; Zaccheo, S. Application of emerging monitoring techniques at the Illinois Basin−Decatur Project. *Int. J. Greenhouse Gas Control* **2020**, *103*, No. 103188.

(7) NETL. Safe geologic storage of captured carbon dioxide: two decades of DOE's carbon storage R&D program in review, 2020.

(8) Takuya, H.; Shinya, K.; Masayuki, I.; Tatsuya, T.; Daisuke, S.; Shimpei, K. MHI's Commercial Experiences with CO2 Capture and Recent R&D Activities. *Mitsubishi Heavy Ind. Techn. Rev.* **2018**, *55* (1), 31−37.

(9) Nediljka, G. M.; Karolina, N. M.; Matej, M. Carbon Capture and Storage (CCS): Technology, Projects and Monitoring Review. *Min.-Geol.-Petrol. Eng. Bull.* **2018**, 1−15.

(10) Huazhou, H.; Yuantao, S.; Chang Xiantong, W.; Zhengqing, L. M.; Shulei, Q. Experimental investigation of pore characteristics and permeability in coal-measure sandstones in Jixi Basin, China. *Energies* **2022**, *15* (16), 5898.

(11) Rice, D. D.; Claypool, G. E. Generation, accumulation, and resource potential of biogenic gas. *AAPG Bull.* **1981**, *65* (1), 5−25.

(12) Coleman, D. D.; Liu, C. L.; Riley, K. M. Microbial methane in the shallow Paleozoic sediments and glacial deposits of Illinois, USA. *Chem. Geol.* **1988**, *71* (1−3), 23−40.

(13) Ehhalt, D. H. The atmospheric cycle of methane. *Tellus* **1974**, *26* (1−2), 58−70.

(14) Huang, H.; Wu, Z.; Bi, C. *Abnormal Characteristics of Component Concentrations in Near-Surface Soil Gas over Abandoned Gobs: A Case Study in Jixi Basin, China*; Natural Resources Research, **2024**.

(15) Han, Z.; Gao, X.; Zhao, H.; et al. Extracellular and intracellular biomineralization induced by Bacillus licheniformis DB1−9 at different Mg/Ca molar ratios. *Minerals* **2018**, *8* (12), 585.

(16) Yangli, P.; Huazhang, Z.; Qinzheng, Y.; et al. Progress in microbial and enzyme immobilization of carbon dioxide. *Chem. Bioeng.* **2010**, *27* (7), 10−13.
(17) Melzer, L. S. *Carbon dioxide enhanced oil recovery (CO2 EOR): Factors involved in adding carbon capture, utilization and storage (CCUS) to enhanced oil recovery*; Center for Climate and Energy Solutions, 2012; pp 1−17.
(18) Sinan, L.; Liwei, Z.; Xuebin, S.; et al. Review on modeling and parameter selection for chemical reactions of mineral dissolution and precipitation under the condition of CO2 sequestration in saline aquifers. *Water Resour. Hydropower Eng.* **2020**, *51* (11), 13−22.
(19) Lowenstam, H; Weiner, S. Mineralization by organisms and the evolution of biomineralization; proceedings of the Biomineralization and Biological Metal Accumulation[C]//Biological and Geological Perspectives Papers presented at the Fourth International Symposium on Biomineralization, Renesse; Springer: The Netherlands, 1982.
(20) Heping, X.; Shihua, R.; Yachen, X.; et al. Development op portunities of the coal industry towards the goal of carbon neut rality. *J. China Coal Soc.* **2021**, *46* (7), 2197−2211.
(21) Kaizhong, Z.; Yuanping, C.; Wei, L.; et al. Influence of supercritical CO2 on pore structure and functional groups of coal: Implications for CO2 sequestration. *J. Nat. Gas Sci. Eng.* **2017**, *40*, 288−298.
(22) Barua, S.; Zakaria, B. S.; Chung, T.; et al. Microbial electro lysis followed by chemical precipitation for effective nutrients re covery from digested sludge centrate in WWTPs. *Chemical Engineering Journal* **2019**, *361*, 256−265.
(23) Qiao, J.; Du, F.; Wang, S.; Tan, F.; Zhang, Y. Enrichment and Occurrence of Mn in 5−2 Coal from Qinglongsi Coal Mine, Northern Ordos Basin. *China. ACS omega.* **2020**, *5* (32), 20202−20214.
(24) Li, Y.; Qin, T.; Liang, Z.; Zheng, C. Oil Has a Higher Methanogenic Potential than Coal in an Oil-Bearing Coal Seam. *ACS omega.* **2023**, *8* (26), 23880−23888.
(25) Ai, C.; Wang, S.; Sun, P.; Zhao, S.; Mu, X. Analysis of the Formation Mechanism of Hydrogen Sulfide in the 13# Coal Seam of Sha** Coal Mine. *ACS omega.* **2024**, *9* (2), 2980−2987. Jan 3;

https://doi.org/10.1021/acsomega.4c04022
ACS Omega 2024, 9, 40559−40565